

Electrohydrodynamically Coupled Minimum Film Boiling in Dielectric Liquids

T. B. Jones* and R. C. Schaeffer†

Colorado State University, Fort Collins, Colo.

The Zuber hypothesis for the minimum film boiling point as a hydrodynamic condition is modified to account for the effects of strong electrohydrodynamic coupling at the vapor-liquid interface surrounding a heated cylindrical wire when the interface is stressed by a strong nonuniform electric field. Different models for ac voltage highly insulating and ac/dc conducting fluid cases are proposed, based on charge relaxation effects. The models predict the effect of electrohydrodynamic coupling on dominant unstable wavelengths and heat flux values at the minimum film boiling condition. The ac voltage, highly insulating fluid model compares favorably with theory. The dc data do not deviate substantially from the ac data. Further, for both ac and dc voltages above some critical voltage, which depends on the heater wire radius, the appearance of the instability of the vapor film changes drastically, indicating an upper limit on the validity of the electrohydrodynamic model developed.

Nomenclature

a	= thickness of liquid layer
b	= thickness of vapor film
\vec{E}	= electric field
\vec{F}^e	= electrical body force
f	= electric field frequency
f_m	= mechanical frequency
g	= gravitational acceleration (9.81 m/sec^2)
j	= $\sqrt{-1}$
k	= $2\pi/\lambda$ = wavenumber
k_y, k_z	= components of wavenumber
p	= pressure
(q/A)	= heat flux
R	= heated wire radius
R'	= $R[\rho_l g / \gamma]^{1/2}$ = dimensionless radius
t	= time
\vec{v}	= fluid velocity
x, y, z	= coordinate axes
α	= $-j\omega$ = growth rate
α_d	= maximum growth rate
γ	= surface tension of liquid
ϵ	= dielectric permittivity
ϵ_0	= permittivity of free space ($8.85 \cdot 10^{-12} \text{ F/m}$)
λ	= wavelength
ξ	= surface displacement
ρ_l	= liquid density
ρ_v	= vapor density
σ	= liquid electrical conductivity
τ_x, τ_r	= electrical surface traction
τ_σ	= charge relaxation time
Φ	= electric potential function
ω	= radian frequency
α_d, λ_d , etc.	= normalized quantities

Presented as Paper 75-690 at the AIAA 10th Thermophysics Conference, Denver, Colo., May 27-29, 1975; submitted July 26, 1976; revision received Sept. 20, 1976. The data reported in this paper were obtained by R. C. Schaeffer in the course of his M.S. thesis research program. The authors gratefully acknowledge the assistance of G.W. Bliss and G.C. Vashinder, who assisted in fabrication of experimental apparatus. Communications with J.H. Leinhard and J.R. Melcher proved very valuable. This work was supported by the Division of Engineering of the National Science Foundation, grants #GK-37398 and #ENG74-12113.

Index categories: Hydrodynamics; Wave Motion and Sloshing.

*Associate Professor of Electrical Engineering, Dept. of Electrical Engineering. Member AIAA.

†Graduate Assistant, Dept. of Electrical Engineering.

Introduction

GENERAL agreement exists as to the effects of electrohydrodynamic (EHD) forces on convective, nucleate, and film boiling heat transfer. Data representative of the experimental results of most workers, showing the effect of these forces on normal pool boiling, are shown in Fig. 1. Though all regimes of EHD coupled heat transfer in liquids have been studied, EHD enhanced film boiling seems to have received the least attention in past experimental and theoretical work. This paper reports progress on an experimental and theoretical investigation into electrohydrodynamically coupled film boiling heat transfer. Specifically, the effects of strong, nonuniform electric fields on the minimum film boiling point are considered. A theory, which predicts the effect of EHD forces on the minimum film boiling point is developed. This theory is based on the well-known Zuber hypothesis^{1,2} concerning minimum film boiling but modified to account for electrohydrodynamic coupling at the vapor-liquid interface. Experimental data are presented as a test of this electrohydrodynamic theory, but further, as an indication of the validity of certain models of the electrostatic field distribution.

Only a few attempts to model true ebullient processes (nucleate and film boiling) have been made. Choi³ and Bonjour, et al.,⁴ correlated the effect of a nonuniform electric field on the boiling crisis with the dielectrophoretic force

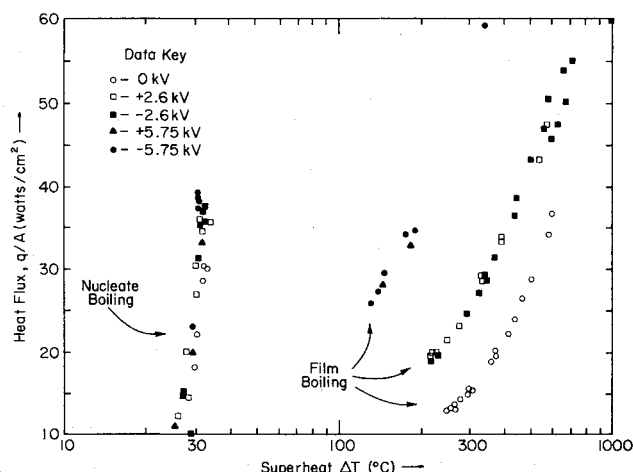


Fig. 1 Pool boiling data showing influence of a dc electric field on boiling in Freon-113[®] with a 0.0127 cm radius platinum wire.

which acts on vapor bubbles. Johnson⁵ considered the electrohydrodynamically coupled surface dynamics of 1) vapor-liquid jets for boiling crisis and 2) vapor films for minimum film boiling. No other truly distinguishable attempts at theoretical modeling of the problem of EHD enhanced boiling heat transfer are found in the literature.

Experimental studies of EHD coupled film boiling have been undertaken by Choi,³ Bonjour et al.,⁴ Johnson,⁵ and Markels and Durfee.^{6,7} All the aforementioned experimentalists have found that the minimum film boiling heat flux is increased by strong electric fields. Further, Markels and Durfee report unique high voltage circuit electric current measurements, which provide some clues as to the influence of the electrohydrodynamic forces on the stable vapor film. Their data indicate a possible electric field dependent intermittent wetting of the heated surface.

The work previously reviewed falls short of providing a complete picture of EHD coupled film boiling on several accounts. First, in theoretical work there is a general lack of recognition of potentially significant differences between ac and dc electric field effects due to charge relaxation. Second, the experiments performed have not been designed with enough of the relevant physical parameters (such as dielectric charge relaxation time, electric field frequency, heater wire radius) in mind. Third, Johnson,⁵ who recognizes the EHD surface coupling mechanism, does not consider the significant effect of the nonuniform electric fields on the dynamics of the vapor-liquid interface.

Theory

Review of the Zuber Theory (no EHD coupling)

Film boiling is characterized by the presence of a vapor film which blankets the heated surface and which essentially prevents liquid from contacting it. This equilibrium is subject to the classical Rayleigh-Taylor instability, which deforms the interface in wave-like corrugations and results in bubbles which carry the heat away from the surface. As the heat flux is turned down, a minimum point is reached at which the heat flux just balances the rate of generation of bubbles due to the Rayleigh-Taylor instability. Zuber hypothesizes that this condition corresponds to the minimum film boiling point.^{1,2} If the heat flux is then further decreased, the instability removes vapor faster than it can be generated and the vapor film collapses.

The basis of the Rayleigh-Taylor instability is the surface equation of motion which results in a dispersion relation⁸ relating stable or unstable wavelengths to frequencies or growth rates. Using empirical results to relate growth rates to bubble release frequencies, it may be shown that, for a flat plate heater,

$$(q/A)_{\min} \propto \lambda_d \alpha_d \quad (1)$$

where α_d is the maximum unstable growth rate and λ_d is the wavelength associated with this maximum growth rate (called the fastest growing wavelength). In the absence of EHD coupling,

$$\lambda_{d0} = 2\pi \left[\frac{3\gamma}{\rho_l g} \right]^{1/2} \quad (2)$$

$$\alpha_{d0} = \left[\frac{2g}{3} \left(\frac{\rho_l g}{3\gamma} \right)^{1/2} \right]^{1/2} \quad (3)$$

For the thin heated wires ordinarily used in pool boiling studies, the minimum film boiling point correlation based upon Eqs. (1-3) is not satisfactory. Therefore Lienhard and Wong⁹ developed a quasi-two-dimensional model which accounts for the effects of transverse curvature on the surface dynamics of a cylindrical vapor film surrounding a wire. This

model successfully predicts the influence of the heated wire radius on the dominant unstable wavelength and the heat flux at the minimum film boiling point. For the cylindrical case⁹

$$\lambda'_{d0} = 2\pi \left[\frac{\rho_l g}{3\gamma} + \frac{1}{6R^2} \right]^{-1/2} \quad (4)$$

$$\alpha'_{d0} = \left[\frac{2g}{3} \left(\frac{\rho_l g}{3\gamma} + \frac{1}{6R^2} \right)^{1/2} \right]^{1/2} \quad (5)$$

where Eqs. (4) and (5) reduce respectively to Eqs. (2) and (3) in the limit of $R \rightarrow \infty$. Using an approach analogous to that of Zuber, Lienhard and Wong⁹ derived a minimum film boiling point heat flux which differs from the proportionality of Eq. (1). This new relationship⁹ predicts that $(q/A)_{\min}$ depends on the second power of the wavelength λ_d ,¹⁰

$$(q/A)_{\min} \propto \lambda_d^2 \alpha_d \quad (6)$$

Based upon theoretical and experimental results reported in this paper, the validity of Eq. (6) is questioned.

Electroquasistatic Regimes of Interest

Depending on the charge relaxation time of the liquid τ_σ , the frequency of the applied electric field f , and the mechanical frequency of the interface, f_m , at least three possible regimes of operation may be hypothesized. The necessary conditions for these three regimes are outlined here.

If the frequency of the electric field is significantly greater than the inverse charge relaxation time, that is,

$$f > 1/\tau_\sigma = \sigma/\epsilon \quad (7)$$

then no charge can build up on the vapor-liquid interface, and a perfectly insulating liquid assumption ($\sigma=0$) is valid for EHD surface wave modeling purposes.¹¹ Under these conditions, the electric field is radially distributed through the vapor and dielectric field.

If the fluid is sufficiently conductive, then the electric field is *totally* excluded from the dielectric fluid. With the entire voltage drop thus occurring across the thin vapor film, the electric field coupling at the vapor-liquid interface is much stronger than that for the highly insulating ac case previously discussed.

An intermediate situation may be hypothesized if the fluid is very highly insulating and if the fundamental mechanical frequency f_m is much greater than the inverse charge relaxation time, i.e.

$$f_m > (\sigma/\epsilon) \quad (8)$$

In this case, the charge at the surface can respond to tangential electric fields quite rapidly, effectively resulting in a conducting interface, with insulating liquid on one side and insulating vapor on the other side.¹² Attempts to use this model in the prediction of EHD coupling effects with insulating dielectric liquids and dc applied voltages have not met with any success.

The three distinct cases previously described briefly represent three important possible electroquasistatic regimes. However, other situations may possibly exist. Some evidence of breakdown in the vapor film for large dc electric fields exists.¹³ In such a case, the electric field distribution would

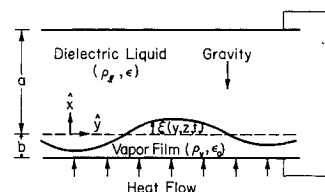


Fig. 2 Flat plate problem geometry.

differ markedly from any of the cases described above. The proper choice amongst these and other electroquasistatic regimes for the modeling of electrohydrodynamic film boiling processes must be based in large part on experimental evidence.

Flat Plate Problem

All the experiments described in this paper involve a thin cylindrical heated wire, but the modeling of the simpler flat plate problem is presented here because the thin cylindrical wire geometry theory is based on this model.

Refer to Fig. 2. The lower plate serves as an electrode and as the heated surface. A thin vapor film of thickness b covers this surface while the liquid layer is of thickness a . It is assumed that

$$b < \lambda < a \quad (9)$$

where λ is the wavelength of disturbances on the vapor-liquid interface. The voltage applied between the upper and lower plates creates an initial uniform electric field which is normal to the interface. It is assumed that the fluid is incompressible, homogeneous, and inviscid, and that the electrostatic approximation is valid. Further, due to the very low relative density of the vapor film, its dynamics are neglected (that is, $\rho_v = 0$). The relevant equations are

$$\rho_l (d\vec{v}/dt) = -\nabla p - \rho_l g \hat{x} + \vec{F}^e \quad (10)$$

$$\nabla \cdot \vec{v} = 0 \quad (11)$$

$$\vec{E} = -\nabla \Phi \quad (12)$$

where \vec{F}^e is the electrical force density including free charge and polarization forces,¹⁴

$$\vec{F}^e = \rho_f \vec{E} - (E^2/2) \nabla \epsilon \quad (13)$$

Electrostriction is not effective due to the incompressibility assumption.¹⁵

The vapor-liquid interface is deformed into wave-like corrugations; the form of this deformation is

$$\xi(y, z, t) = \text{Re} \{ \hat{\xi}(t) e^{-j(k_y y + k_z z)} \} \quad (14)$$

If the deformation is small enough,

$$|\xi(y, z, t)| < b \quad (15)$$

from which a linearized theory for small amplitude surface waves may be developed. The assumptions of fluid incompressibility and homogeneity indicate that the electromechanical interaction may be completely accounted for by a balance of hydrodynamic and hydrostatic pressures with the surface tension and electrical surface forces at the in-

terface. The details of the fluid mechanical and electroquasistatic boundary value problems are not covered here. The balance of forces to first order in $\xi(y, z, t)$ at the vapor-liquid interface results in a surface equation

$$\frac{\rho_l}{k} \cdot \frac{d^2 \hat{\xi}}{dt^2} + k^2 \gamma \hat{\xi} - \rho_l g \hat{\xi} - \tau_x(\hat{\xi}, V) = 0 \quad (16)$$

where $k^2 = k_x^2 + k_y^2$, and $\tau_x(\hat{\xi}, V)$ is the normally acting electrical surface traction. The form of τ_x depends on which electroquasistatic condition discussed in the preceding subsection is in force. Refer to Table 1 where expressions for τ_x are contained. Equation (16) is parametric in $V(t)$, the applied voltage, but it is found from experiment that the important mechanical frequencies are in a range from 10 to 30 Hz. Since the lowest attainable ac voltage frequency in the experiments reported is 45 Hz, parametric effects are not likely to occur, and thus they are neglected.

If parametric effects can be neglected, then all dependent variables can be assumed to have sinusoidal dependence, e.g.,

$$\hat{\xi}(t) = \hat{\xi} e^{j\omega t} \quad (17)$$

and the surface equation may be reduced to a dispersion equation relating ω and k . Table 1 contains the normalized dispersion relations for two of the three electroquasistatic regimes. Note that the following convenient normalizations have been used

$$\underline{k} = k/k_{d0} \quad (18)$$

$$\underline{\omega} = \omega/\alpha_{d0} \quad (19)$$

The dispersion relations show that the surface tension tends to stabilize, while the gravitational and electrohydrodynamic terms tend to destabilize the interface. In the zero-voltage limit, the Rayleigh-Taylor instability emerges. Note also that the interface is always unstable for very small k (very large wavelength λ). The unstable wavelength λ_d with the fastest growth rate $\alpha_d = (-j\omega)_{\max}$ is important in the minimum film boiling point theory, and normalized expressions for these important quantities are included in Table 1. These quantities are normalized to their zero-EHD coupled values, λ_{d0} and α_{d0} .

From Eq. (1),

$$\frac{(q/A)_{\min}}{(q/A)_{\min 0}} = \frac{\lambda_d}{\lambda_{d0}} \cdot \frac{\alpha_d}{\alpha_{d0}} \quad (20)$$

Table 1 shows that the electric field tends to decrease wavelength while increasing the growth rate. Thus, the relative effects of the electric field on λ_d and α_d determine the net effect on the minimum film boiling point heat flux. Equation (20) neglects the effect of the zero-order electrical

Table 1 Summary of theoretical results for the Flat Plate Problem ($ka \gg 1$, $kb \ll 1$, $\rho_l \gg \rho_v$ assumed)

PHYSICAL MODEL	EHD SURFACE TRACTION (τ_x)	EHD INFLUENCE NUMBER (El)	DISPERSION RELATION (NORMALIZED)	NORMALIZED FASTEST GROWING WAVELENGTH ($\lambda_d = \lambda_d/\lambda_{d0}$)	NORMALIZED MAXIMUM GROWTH RATE ($\alpha_d = \alpha_d/\alpha_{d0}$)
(i) INSULATING FLUID, AC FIELD	$\epsilon \left(\frac{\epsilon}{\epsilon_0} - 1 \right)^2 \frac{V^2 k}{a^2} \hat{\xi}$	$\epsilon \left(\frac{\epsilon}{\epsilon_0} - 1 \right)^2 \frac{V^2}{4a^2 \sqrt{\rho_l g \gamma / 3}}$	$\underline{\omega}^2 = \frac{1}{2} \underline{k}^3$ $-\frac{3}{2} \underline{k} - El \cdot \underline{k}^2$	$\left\{ \frac{2}{3} El + \left[\frac{4El^2}{9} + 1 \right]^{1/2} \right\}^{-1}$	$\left\{ \underline{\lambda}_d^{-1} + El/3 \right\}^{1/2}$
(ii) CONDUCTING FLUID, AC/DC	$\epsilon_0 \frac{V^2}{b^3} \hat{\xi}$	$\frac{3 \epsilon_0 V^2}{2 \rho_l g b^3}$	$\underline{\omega}^2 = \frac{1}{2} \underline{k}^3$ $-\left(\frac{3}{2} + El \right) \underline{k}$	$\left\{ 1 + \frac{2}{3} El \right\}^{-1/2}$	$\left\{ 1 + \frac{2}{3} El \right\}^{3/4}$

Table 2 Summary of theoretical results for the Cylindrical Heated Wire Problem ($b \ll R \ll R_0$, $\rho_l > \rho_v$ ($g^* = g + \gamma/2\rho_l R^2$))

PHYSICAL MODEL	ELECTROHYDRODYNAMIC SURFACE TRACTION (τ_x)	ELECTROHYDRODYNAMIC INFLUENCE NUMBER ($E\ell$)	DISPERSION RELATION (NORMALIZED)	NORMALIZED MOST DANGEROUS WAVELENGTH ($\lambda_d = \lambda_d'/\lambda_{d0}$)	GROWTH RATE OF MOST DANGEROUS WAVELENGTH ($\alpha_d = \alpha_d'/\alpha_{d0}$)
(1) INSULATING FLUID, AC FIELD	$\frac{\epsilon(\frac{\epsilon}{\epsilon_0}-1)\left[1+(\frac{\epsilon}{\epsilon_0}-1)kR\right]V^2\hat{\xi}}{4R^3\left[\ln\left(\frac{R_0}{R}\right)\right]^2}$	$\frac{3\epsilon(\frac{\epsilon}{\epsilon_0}-1)V^2}{8\rho_l g^* R^3\left[\ln\left(\frac{R_0}{R}\right)\right]^2}$	$\frac{\omega^2}{k^3} = \frac{1}{2}k^3 - \frac{3}{2}k - E\ell k$ $-\left(\frac{\epsilon}{\epsilon_0}-1\right)k_{d0}RE\ell k^2$	$\left\{\frac{2}{3}E\ell' + \left[\left(\frac{2}{3}E\ell'\right)^2 + \frac{2}{3}E\ell + 1\right]^{\frac{1}{2}}\right\}^{-1}$	$\left\{\lambda_d^{-1} + \frac{2}{3}\lambda_d^{-1}E\ell + \frac{1}{3}\lambda_d^{-2}E\ell'\right\}^{\frac{1}{2}}$
(11) CONDUCTING FLUID, AC/DC	$\frac{\epsilon_0 V^2 \hat{\xi}}{4b^3}$	$\frac{3\epsilon_0 V^2}{8\rho_l g^* b^3}$	$\frac{\omega^2}{k^3} = \frac{1}{2}k^3 - \left(\frac{3}{2} + E\ell\right)k$	$\left\{1 + \frac{2}{3}E\ell\right\}^{-\frac{1}{2}}$	$\left\{1 + \frac{2}{3}E\ell\right\}^{\frac{3}{4}}$

$$^a E\ell' = \left(\frac{\epsilon}{\epsilon_0} - 1\right)k_{d0}'RE\ell$$

surface traction on the vapor density, which is calculated to be small.

Comparison of the dispersion relations in Table 1 shows that for a given applied voltage V , the dc, highly conducting fluid case exhibits the strongest electrohydrodynamic coupling, while the ac, highly insulating fluid case exhibits the weakest EHD coupling. The thickness of the vapor film $b \ll a$ plays the crucial role in establishing the more intense normal electric field at the vapor-liquid interface for the conducting fluid case. Accurate predictions of b are important in any calculations of $(q/A)_{\min}$ for this case, but not for the insulating fluid case.

Equation (20), with the ac, highly insulating expressions for λ_d and α_d from Table 1, checks with Johnson's similar expression (his Eq. (19)).⁵

Thin Cylindrical Wire Problem

The model for the electrohydrodynamically enhanced thin heated wire pool boiling experiment is essentially a modification of the theory of Lienhard and Wong.⁹ Their theory is a quasi-two-dimensional modification of Zuber's theory, developed to account for the transverse curvature of the vapor-liquid interface. In turn, the modification presented here adds in the effect of a nonuniform normal electric field. The approach followed is to add the nonuniform electric field and transverse surface curvature terms to the surface equation of motion.

Lienhard and Wong⁹ rely upon experimental observations of the vapor film deformation for their modeling exercise. The basis of their simplified quasi-two-dimensional model is that the vapor film deforms and releases bubbles only on the top surface as shown in Fig. 3. For electric fields up to moderate values, this observation is still valid, and so a relatively straightforward modification to the flat plate theory of the preceding subsection is possible.

The surface equation for the small surface deformations

$$\xi(z, t) = \text{Re}[\hat{\xi}(t)e^{-jkz}] \quad (21)$$

is

$$\frac{\rho_l}{k} \cdot \frac{d^2 \hat{\xi}}{dt^2} + \gamma(k^2 - \frac{1}{2R^2})\hat{\xi} - \rho_l g \hat{\xi} - \tau_r(\hat{\xi}, V) = 0 \quad (22)$$

The surface tension term now includes both longitudinal stabilizing and transverse destabilizing components. The circumferentially averaged normal electric surface traction τ_r includes components due to the self-field and electric field gradient effects, both of which are destabilizing. The surface traction expressions for two of the three electroquasistatic cases in the preceding subsection are found in Table 2.

The dispersion relations in Table 2 use the normalizations

$$\frac{\omega}{k} = \omega/\alpha_{d0}' \quad (23)$$

$$k = k/k_{d0}'$$

Also found in Table 2 are normalized expressions for the previously defined quantities λ_d and α_d . These dispersion relations reduce to the result of Lienhard and Wong⁹ in the limit of $V=0$. Note the destabilizing nature of both the self-field and the electric field gradient terms.

The obvious differences between the flat plate and cylindrical wire problems are reflected in the different expressions for λ_d and α_d found in Tables 1 and 2. These differences are caused by the net effects of transverse surface curvature and the nonuniform electric field. A more subtle apparent difference appears when the theory of Lienhard and Wong is closely scrutinized. Their Eq. (20) suggests that the minimum film boiling point is proportional to the quantity $\lambda_d^2 \alpha_d$, as reflected in Eq. (6). The theory developed here to account for electrohydrodynamic effects on minimum film boiling relies on predictions of the electric field influence on λ_d and α_d . Thus, if the dependence of $(q/A)_{\min}$ on λ_d and α_d is not correct, then discrepancies between theory and experiment are bound to arise even if the EHD model is correct. The theory using Table 2 with Eq. (6) predicts a monotonic decrease in the minimum film boiling heat flux as the voltage is increased. This is due to the λ_d^2 dependence. If our Eq. (20) is used instead, fairly good experimental correlation is obtained (see following section). The evidence thus indicates that Eq. (6) is not physically correct, and that the Lienhard and Wong's expression for $(q/A)_{\min}$, viz their Eq. (20),⁹ is misleading in form, though parametrically correct in the absence of electrohydrodynamic coupling.

Experiment

Description of Apparatus

The experiment is illustrated in Fig. 4. A thin wire is held securely along the axis of a 6 cm diameter pyrex glass cylinder. A conductive layer of aluminum deposited on the inside

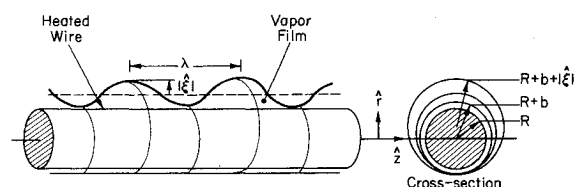


Fig. 3 Cylindrical problem geometry.

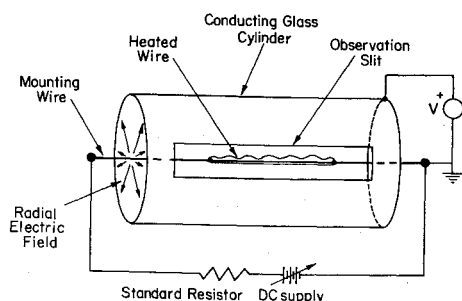


Fig. 4 Cylindrical heated wire experimental apparatus and circuitry.

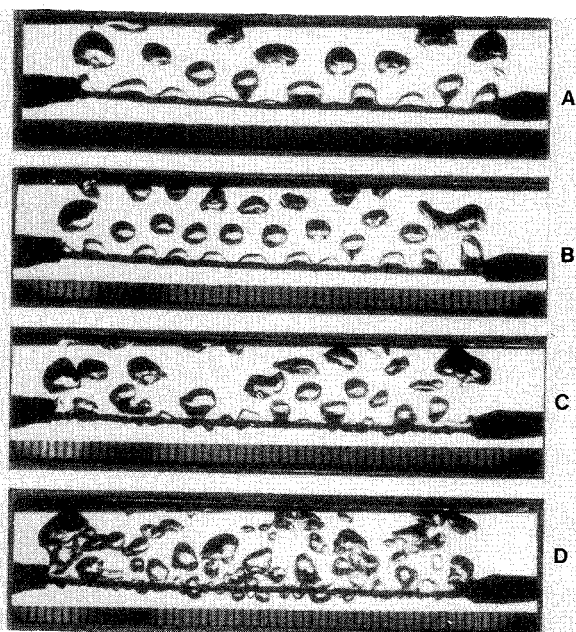


Fig. 5 Minimum film boiling on a horizontal heated wire in Freon-113, nichrome wire (radius = 0.0406 cm). a) $V = 0$ kV, b) $V = 2$ kV, c) $V = 4$ kV, d) $V = 6$ kV.

surface of the glass cylinder serves as an electrode. Thin masked slits on opposite sides of the cylinder provide a convenient means of observing boiling phenomena. These slits are small enough to avoid any electric field distortion. The test wire is soldered to two 16 gage copper wires which are, in turn, fastened to the end bulkheads as shown. Constraints imposed by the electrode configuration make it necessary to provide end fastenings for the heater wire which are subject to end effects as discussed by Kovalev.¹⁶ The glass cylinder assembly with the heater wire in place is immersed in a large pyrex tank filled with the experimental dielectric fluid, Freon-113®. A preheater and mechanical stirrer maintain the fluid outside the cylinder at uniform temperature without introduction of significant fluid convection inside the cylindrical experimental test cell.

For ac electric field experiments, a variable frequency ac power supply is used with a modified X-ray step-up transformer to achieve voltages to 10 kV (rms) at frequencies from 45 to 500 Hz. A 20 kV battery bank provides ripple-free dc voltages for dc experiments. Freon-113® is used exclusively as the experimental heat transfer fluid. The important properties of this dielectric fluid are contained in Table 3. All experiments are run at or very close to saturation conditions for the liquid.

Heater wires of two sizes have been used experimentally. The first is a 0.0127 cm radius platinum wire, and the other is a 0.0406 cm radius nichrome wire. The dimensionless radius R' of Lienhard and Sun¹⁷ is a modulus useful in characterization of these experiments

$$R' = R[\rho_l g / \gamma]^{1/2} \quad (24)$$

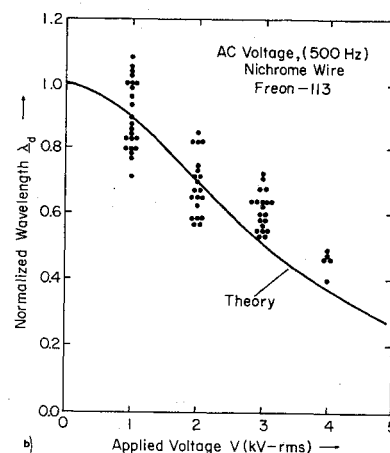
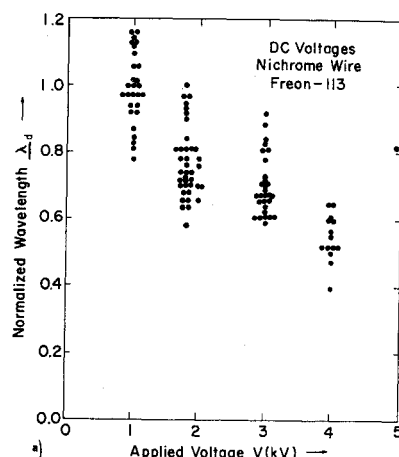


Fig. 6 Normalized wavelength data and theory for nichrome wire (radius = 0.0406 cm) at minimum film boiling point in Freon-113. a) dc voltage, b) ac voltage (500 Hz).

For the platinum wire $R' = 0.12$ and for the nichrome wire $R' = 0.39$, both in Freon-113® at saturation.

Procedure

The experimental data at the minimum film boiling point are obtained as follows. The bath heater and stirrer are turned on and allowed to bring the entire fluid mass up to the saturation temperature. After equilibrium is reached, the voltage is applied to the heated wire and it is turned high enough to obtain the spontaneous transition from nucleate to stable film boiling. Then, the electric field is applied and after a new equilibrium is achieved the heated wire current is decreased slowly toward the minimum film boiling point. Eventually, an equilibrium point is reached at which nucleate boiling starts to emerge at one end of the wire. Just below this point, nucleate boiling starts to propagate down the wire. This point is interpreted as the minimum film boiling condition. At this point, the current and voltage in the heater wire are measured and/or a high-speed photograph of the wire and surrounding vapor film is taken in order to obtain the wavelength data. This same procedure is duplicated to obtain minimum film boiling point data at other applied voltages and frequencies.

Experimental Results

The data plotted in Fig. 1 are obtained from an experiment using a platinum wire and dc voltages of both polarities. These results show the overall qualitative consistency of this experiment with other previous work of Choi³ and Bonjour et al.⁴ Note that the effect on minimum film boiling is to increase $(q/A)_{\min}$ while slightly decreasing the superheat ΔT .

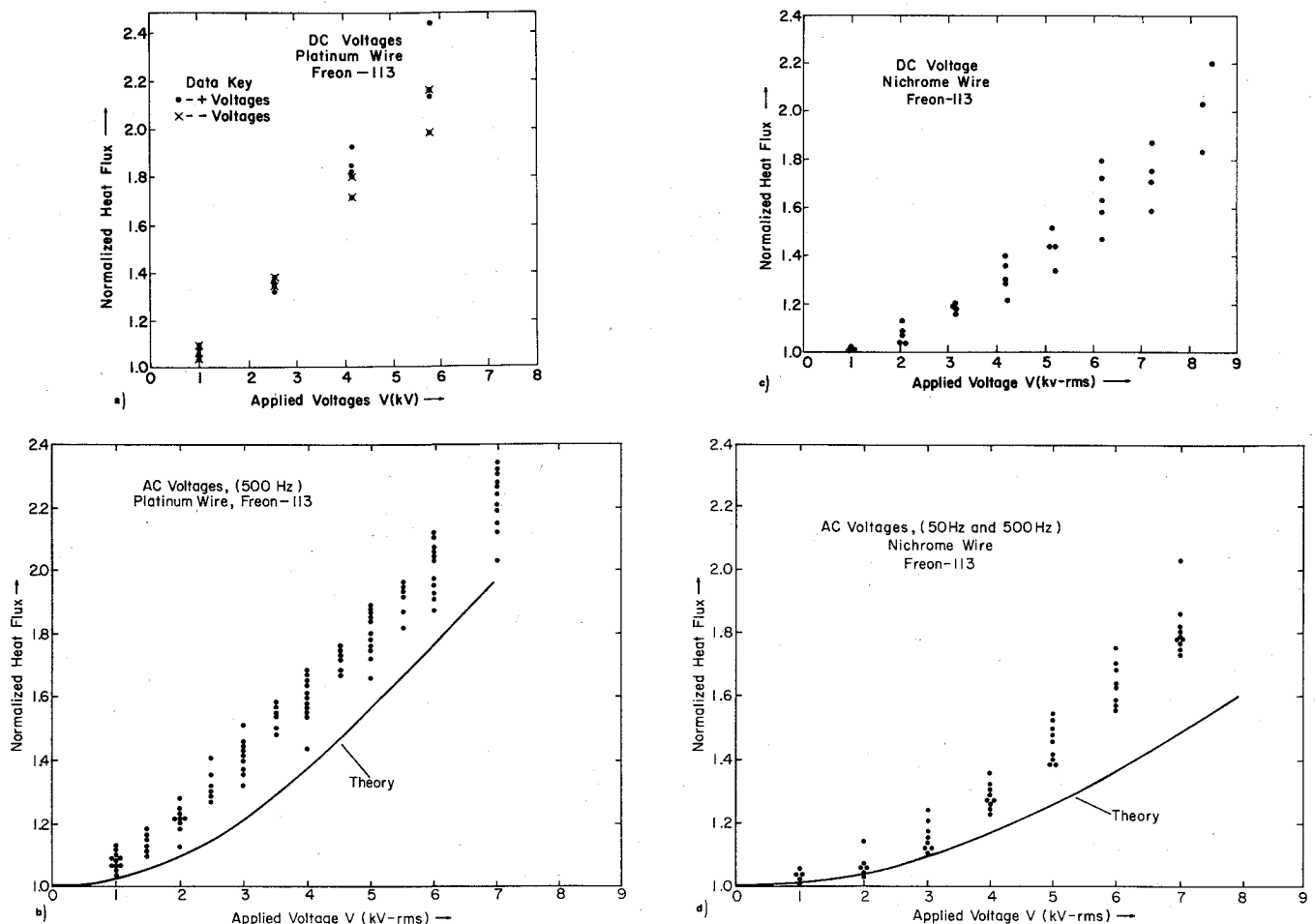


Fig. 7 Normalized minimum film boiling heat flux and theory. a) Platinum wire (radius = 0.0127 cm) dc voltage, b) Platinum wire (radius = 0.0127 cm) ac voltage (500 Hz), c) Nichrome wire (radius = 0.0406 cm) dc voltage, d) Nichrome wire (radius = 0.0406 cm) ac voltage (50 and 500 Hz).

Substantial effort has been devoted to measurements of the dominant unstable wavelength at the minimum film boiling point for both the platinum wire (radius = 0.0127 cm) and the nichrome wire (radius = 0.0406 cm). Much greater success has been encountered with the thicker (nichrome) wire. If any voltage above ~0.5 kV is applied to the thinner wire, serious distortion of the vapor-liquid interface occurs and identification of wavelengths is not possible. A similar effect occurs for voltages above ~4.0 kV for the nichrome wire. Refer to Fig. 5. In these high-speed photographs, the effect of the electric field is quite evident. Initially, as the voltage is increased, the dominant wavelength decreases, but eventually the surface dynamics change drastically. Note that in Figs. 5c and 5d, vapor bubbles start forming on the lower side of the wire. This suggests that the radial symmetry of the electric field starts to dominate the asymmetric nature of the gravitational body force.

The data plotted in Fig. 6a are from experiments conducted with dc electric fields using the thicker (nichrome) wire, and they are normalized to the average of the zero electric field wavelength data points, all of which fall within $\pm 40\%$ of the median of 6.4 cm. The data exhibit scatter, which may be explained partially by the theoretical prediction that a band of wavelengths about λ_d is unstable. No success in the theoretical prediction of this data or for any other dc voltage experiments has been obtained. Several explanations for the lack of success may be offered, including corona breakdown in the vapor film and surface charge pumping near the ends of the heated wire sections.

Figure 6b plots wavelength data obtained again using the nichrome wire with a 500 Hz ac applied electric field. These

data are also normalized to the average of the zero electric field wavelength values. Again, scatter is evident, and the experimental points lie somewhat above the theoretical curve obtained from case (i) of Table 2.

In Fig. 7 are plotted experimental minimum heat flux data for the platinum and nichrome wires and dc and ac (500 Hz) electric fields. These data are normalized similar to the wavelength data. Two-fold increases in the minimum film boiling point are obtained for the platinum wire and the nichrome wire. In Figs. 7b and 7d, theoretical curves from case (i) of Table 2 are plotted along with the data.

Discussion

The ac wavelength data, for which a theory exists, are reasonably consistent with the predictions of the electrohydrodynamic surface wave model. The electric field coupling decreases the dominant unstable wavelength up to some value of voltage where substantial alterations to the interfacial dynamics become apparent, as shown in Fig. 5. Clearly, another more complex model for the vapor-liquid

Table 3 Freon-113[®] properties at saturation conditions

liquid density (ρ_L)	$1.51 \cdot 10^3 \text{ kg/m}^3$
surface tension (γ)	.0159 Nt/m
boiling point	48°C
relative dielectric constant ($\frac{\epsilon}{\epsilon_0}$)	2.33
electrical conductivity (σ)	$<10^{-12} (\Omega\text{-m})^{-1}$

surface deformations is required above this critical voltage. This critical voltage is dependent on the wire radius, suggesting that some electric field parameter measured at the vapor interface is important.

The correlation of the minimum film boiling heat flux data to the theory for case (i) is reasonable for Figs. 7b and 7d. Given the uncertainties in taking minimum film boiling data, such agreement may be fortuitous. Yet the simultaneous good agreement of both the wavelength and heat flux data suggests otherwise. If one accepts the conclusion that the success with the wavelength data validates the electrohydrodynamic model, then the success with the heat flux data means that the Eq. (20) is valid for cylindrical heated wires as well as flat plates.

A forceful argument questioning the validity of the data, based on the uncertain influence of end effects on experimental determination of the actual minimum film boiling condition may be made.^{10,16} However, the method of data presentation is intended to alleviate such objections. The data are normalized to the zero electric field value, and thus Figs. 6 and 7 present only the effects of the electric field on the hydrodynamic and heat transport processes. In this way, various empirical factors discussed by Berenson¹⁸ are presumably eliminated. Since the electric fringing field effects are minimal at the ends of the heated wire, the same electrical forces are in play there as in the center of the heated wire, where the analysis of the Flat Plate Problem subsection applies. Since both the wavelength and heat flux data correlate reasonably well to theory for the ac electric field insulating fluid case (see Figs. 6b and 7d), there appears to be justification for this similarity argument.

The data of Figs. 6a, 7a, and 7c indicate that little difference exists between the ac and dc electrohydrodynamic effects, both in wavelength and minimum film boiling heat flux values. All attempts to model the dc case produced predictions of much stronger coupling. A fundamental lack of understanding of the dc interactions exists. Of the proposed explanations, neither vapor corona breakdown nor surface shear pumping near the ends has yet been conclusively identified.

Conclusion

Some tentative conclusions supported by the previous sections of this paper can be drawn. 1) Good correlation of theory and experimental data exist for ac experiments in an insulating dielectric fluid (Freon-113®). The theory accurately predicts the effect of electrohydrodynamic coupling on dominant unstable wavelengths and minimum film boiling heat flux. 2) The dc experiments do not provide very consistent results and, further, the data do not seem to deviate very much from the ac data. No model to predict the dc electrohydrodynamic surface wave coupling exists. Electroconvection effects not observed for ac and corona breakdown are two mechanisms which may be at work. 3) Electric fields substantially alter the basic Rayleigh-Taylor instability mechanism above some threshold voltage which is dependent upon the heater wire radius. A strictly three-dimensional

model may be required to account for electrohydrodynamic surface coupling above this threshold voltage which is dependent upon the heater wire radius.

The electroquasistatic models for dc electrohydrodynamic coupling in film boiling are not yet verified, due to the presently limited data. Considerable further experimental work is required. More dc voltage wavelength, bubble frequency and heat flux data at the minimum film boiling point must be obtained. Other experimental fluids must also be tried. Further experiments with heater wires of varying sizes will be needed to quantify the effect of voltage and wire size on the hydrodynamics of the vapor-liquid interface.

References

- ¹Zuber, N. and Tribus, M., "Further Remarks on the Stability of Boiling Heat Transfer," UCLA Report #58-5, UCLA, Los Angeles, Calif., Jan. 1958.
- ²Zuber, N., "Hydrodynamic Aspects of Boiling Heat Transfer," AEC Rept. #AECU-4439, June 1959, Atomic Energy Commission.
- ³Choi, H. Y., "Electrohydrodynamic Boiling Heat Transfer," Ph.D. thesis, MIT, Cambridge, Mass., 1962.
- ⁴Bonjour, E., Verdier, J., and Weil, L., "Electroconvection Effects on Heat Transfer," *Chemical Engineering Progress*, Vol. 58, 1962, pp. 63-66.
- ⁵Johnson, R. L., "Effect of an Electric Field on Boiling Heat Transfer," *AIAA Journal*, Vol. 6, 1968, pp. 1456-1460.
- ⁶Markels, M., and Durfee, R. L., "The Effect of Applied Voltage on Boiling Heat Transfer," *AIChE Journal*, Vol. 10, 1964, pp. 106-110.
- ⁷Markels, M., and Durfee, R. L., "Studies of Boiling Heat Transfer with Electric Fields," *AIChE Journal*, Vol. 11, 1965, pp. 716-723.
- ⁸Lamb, H., *Hydrodynamics*, Dover Press, New York, 1945, Sec. 267.
- ⁹Lienhard, J. H., and Wong, P. T. Y., "The Dominant Unstable Wavelength and Minimum Heat Flux During Film Boiling on a Horizontal Cylinder," *Transactions of the ASME: Journal of Heat Transfer*, Vol. 86C, 1964, pp. 220-226.
- ¹⁰Lienhard, J. H., private communications, 1974.
- ¹¹Devitt, E. B., and Melcher, J. R., "Surface Electrohydrodynamics with High-Frequency Fields," *The Physics of Fluids*, Vol. 8, 1965, pp. 1193-4.
- ¹²Melcher, J. R., and Smith, C. V., "Electrohydrodynamic Charge Relaxation and Interfacial Perpendicular-Field Instability," *The Physics of Fluids*, Vol. 12, 1969, pp. 778-790.
- ¹³Schaeffer, R. C., unpublished experimental work, Colorado State University, Fort Collins, Colo., 1973-74.
- ¹⁴Stratton, J. A., *Electromagnetic Theory*, McGraw-Hill, New York, 1941, sec. 2.21.
- ¹⁵Rosenkilde, C. E., "A Dielectric Fluid Drop in an Electric Field," *Proceedings of the Royal Society (London)*, Vol. A312, 1969, pp. 473-494.
- ¹⁶Kovalev, S. A., "An Investigation of Minimum Heat Fluxes in Pool Boiling of Water," *International Journal of Heat and Mass Transfer*, Vol. 9, pp. 1219-1226.
- ¹⁷Lienhard, J. H., and Sun, K. H., "Effects of Gravity and Size upon Film Boiling from Horizontal Cylinders," *Transactions of the ASME: Journal of Heat Transfer*, Vol. 92C, 1970, pp. 292-298.
- ¹⁸Berenson, P. J., "Discussion of 'The Dominant Unstable Wavelength and Minimum Heat Flux during Film Boiling on a Horizontal Wire,'" *Transactions of the ASME: Journal of Heat Transfer*, Vol. 86C, 1964, p. 225.